

SHOULD TYPE IA SUPERNOVA DISTANCES BE CORRECTED FOR THEIR LOCAL ENVIRONMENTS?

D. O. JONES¹, A. G. RIESS^{2,3}, D. M. SCOLNIC^{4,5}, Y.-C. PAN^{6,7,8}, E. JOHNSON², D. A. COULTER¹, K. G. DETTMAN⁹, M. M. FOLEY¹⁰, R. J. FOLEY¹, M. E. HUBER¹¹, S. W. JHA⁹, C. D. KILPATRICK¹, R. P. KIRSHNER^{10,12}, A. REST^{2,3}, A. S. B. SCHULTZ¹¹, M. R. SIEBERT¹

Draft version September 19, 2018

ABSTRACT

Recent analyses suggest that distance residuals measured from Type Ia supernovae (SNe Ia) are correlated with local host galaxy properties within a few kpc of the SN explosion. However, the well-established correlation with global host galaxy properties is nearly as significant, with a shift of 0.06 mag across a low to high mass boundary (the mass step). Here, with 273 SNe Ia at $z < 0.1$, we investigate whether stellar masses and rest-frame $u - g$ colors of regions within 1.5 kpc of the SN Ia explosion site are significantly better correlated with SN distance measurements than global properties or properties measured at random locations in SN hosts. At $\lesssim 2\sigma$ significance, local properties tend to correlate with distance residuals better than properties at random locations, though despite using the largest low- z sample to date we cannot definitively prove that a local correlation is more significant than a random correlation. Our data hint that SNe observed by surveys that do not target a pre-selected set of galaxies may have a larger local mass step than SNe from surveys that do, an increase of 0.071 ± 0.036 mag (2.0σ). We find a 3σ local mass step after global mass correction, evidence that SNe Ia should be corrected for their local mass, but we note that this effect is insignificant in the targeted low- z sample. Only the local mass step remains significant at $> 2\sigma$ after global mass correction, and we conservatively estimate a systematic shift in H_0 measurements of -0.14 km s⁻¹Mpc⁻¹ with an additional uncertainty of 0.14 km s⁻¹Mpc⁻¹, $\sim 10\%$ of the present uncertainty.

1. INTRODUCTION

Type Ia supernovae (SNe Ia) have become increasingly precise cosmological distance indicators through improvements in how they are standardized. Beyond accounting for the light-curve shape and color of SNe Ia, the most recent and smallest effect to be routinely addressed in cosmological samples is a ~ 0.06 mag correction derived from the empirical correlation of SNIa distance residuals with host galaxy mass (the mass step; Kelly et al. 2010; Lampeitl et al. 2010; Sullivan et al. 2010). Cosmology analyses typically correct for the mass step (Sullivan et al. 2011; Betoule et al. 2014) despite a lack of understanding of the underlying cause. If mass serves only as a proxy for the underlying cause, for example, metallicity or progenitor age (Hayden et al. 2013; Chil-

dress et al. 2014; Graur et al. 2015), a somewhat different correction may yield improved cosmological distance estimates from SNe Ia.

In cases where the progenitor has a short delay between formation and explosion (prompt SNe Ia), the environment near the site of the SN could be used as a better diagnostic of the properties of the progenitor than the global host environment. Up to 50% of SNe Ia could explode less than 500 Myr after the formation of their progenitor systems (Rodney et al. 2014; Maoz et al. 2014). Therefore, a correction based on the local environment may be a better method of standardizing SNe Ia than a correction based on the host galaxy as a whole. However, for SNe Ia with longer delay times such a correlation becomes less likely.

Evidence for a correlation between SN shape- and color-corrected magnitude (hereafter corrected magnitude) and local star formation rate within 1-2 kpc of the SN explosion site was reported by Rigault et al. (2013) using SN Factory data (Aldering et al. 2002) and Rigault et al. (2015) for a publicly available SN sample (Hicken et al. 2009a). Kelly et al. (2015) found evidence that the dispersion of SN corrected magnitudes was lower in highly star-forming local environments but had only a small sample of ~ 20 SNe that were found in such environments. However, Jones, Riess, & Scolnic (2015) found that after applying updated light curve fitters and employing the same sample selection as used for cosmological analyses, the relationship between inferred SNIa distance and local star formation was found to be insignificant in a sample of 179 $z < 0.1$ SNe Ia.

More recently, Roman et al. (2018) examined the relationship between SN corrected magnitude and local, rest-frame $U - V$ color. A “step” between blue and red colors was seen at 1.7σ significance at $z < 0.1$ and

¹ Department of Astronomy and Astrophysics, University of California, Santa Cruz, CA 92064, USA

² Department of Physics and Astronomy, The Johns Hopkins University, Baltimore, MD 21218

³ Space Telescope Science Institute, Baltimore, MD 21218

⁴ University of Chicago, Kavli Institute for Cosmological Physics, Chicago, IL, USA

⁵ Hubble, KICP Fellow

⁶ Division of Theoretical Astronomy, National Astronomical Observatory of Japan, 2-21-1 Osawa, Mitaka, Tokyo 181-8588, Japan

⁷ Institute of Astronomy and Astrophysics, Academia Sinica, Taipei 10617, Taiwan

⁸ EACOA Fellow

⁹ Department of Physics and Astronomy, Rutgers, The State University of New Jersey, 136 Frelinghuysen Road, Piscataway, NJ 08854, USA

¹⁰ Harvard-Smithsonian Center for Astrophysics, 60 Garden Street, Cambridge, MA 02138, USA

¹¹ Institute for Astronomy, University of Hawaii, 2680 Woodlawn Drive, Honolulu, HI 96822, USA

¹² Gordon and Betty Moore Foundation, 1661 Page Mill Road, Palo Alto, CA 94304, USA

6.9 σ significance when using SNe Ia from $0.1 < z < 0.5$ (and 7.0 σ significance when all SNe are included). The $z < 0.1$ step measurement is 0.053 ± 0.032 mag, while the $0.1 < z < 0.5$ step is 0.117 ± 0.017 mag. The reason for this difference is unclear. Factors could include statistical fluctuation, survey selection effects, different effective apertures due to blending at high- z , or a redshift-dependent local step. Similarly, Kim et al. (2018) used global properties to *infer* local properties for a subset of SNe Ia from $0.01 \lesssim z \lesssim 1$, finding that the inferred local star formation correction was 0.081 ± 0.018 mag, 0.024 mag larger than the global mass step. Rigault et al. (2018) recently measured a 0.163 ± 0.029 mag correlation between local *specific* star formation rate (sSFR) and Hubble residual using SNFactory data but do not measure a global sSFR step. Uddin et al. (2017) also examined 1338 SN Ia and found that SNe Ia in host galaxies with high *global* sSFR had the lowest intrinsic dispersion of the subsamples they examined.

Here, we ask whether the evidence for a local step implies that host galaxy properties near the SN location contain additional information that could improve the standardization of SNe Ia. Alternatively, it may be that local regions merely trace global host galaxy properties. Roman et al. (2018), for example, found that the size of the local step decreases by just 0.022 mag when inferring local properties within an aperture of radius 16 kpc, an aperture that should contain nearly all the light from a galaxy. With the first data release of the Foundation low- z SN sample (Foley et al. 2018), we are now able to ask this question with up to 273 $z < 0.1$ SNe Ia, a low- z sample that is $\sim 40\%$ larger than that used in previous cosmological analyses (Scolnic et al. 2018; Jones et al. 2018; Betoule et al. 2014).

We use measurements of the stellar mass and local, rest-frame $u - g$ colors near the SN location. The local stellar mass is a natural first measurement to investigate, given the known correlation of SN distance residuals with global stellar mass. Measuring local stellar mass is also a convenient measurement; it only requires optical photometry, which is available for the entire low- z SN sample. Rest-frame $u - g$ colors, on the other hand, are effectively the same as the local $U - V$ colors used by Roman et al. (2018). $u - g$ colors are sensitive to the host galaxy star formation without suffering from the resolution limitations of shorter-wavelength UV instruments such as GALEX (e.g. Jones et al. 2015).

We measure the Hubble residual “step” as a function of global properties, local properties, and the properties within 1.5 kpc apertures at random locations within each host galaxy. In §2 we present the SN sample and we measure host galaxy properties in §3. In §4 we measure the correlation of these data with host galaxy properties, and in §5 we examine the impact of our results on the Hubble constant. We conclude in §6.

2. DATA AND ANALYSIS

For this analysis, we combine 216 $z < 0.1$ SNe from the Pantheon compilation (Scolnic et al. 2018) with 178 SNe Ia from the Foundation first data release (DR1; Foley et al. 2018). This combined sample contains 394 SNe Ia and twice as many SNe Ia at $z < 0.1$ as recent cosmological analyses (e.g. Scolnic et al. 2018).

The Pantheon compilation includes SNe observed by

CfA surveys 1-4 (Riess et al. 1999; Jha et al. 2006; Hicken et al. 2009b,a, 2012) and the Carnegie Supernova Project (Contreras et al. 2010; Folatelli et al. 2010; Stritzinger et al. 2011). It also includes 43 $z < 0.1$ SNe discovered by SDSS (Kessler et al. 2009) and PS1 (Scolnic et al. 2018; Rest et al. 2014; Scolnic et al. 2014b).

The Foundation survey uses the Pan-STARRS1 (PS1) telescope to follow nearby SNe Ia discovered by ASAS-SN (Holoien et al. 2017), ATLAS (Tonry et al. 2018), Gaia (Gaia Collaboration et al. 2016), and the Pan-STARRS Survey for Transients (PSST; Huber et al. 2015) among other surveys. SNe Ia from the Foundation DR1 are observed on the well-calibrated PS1 photometric system (Schlafly et al. 2012) and can therefore be used to measure distances with good control over systematic uncertainties. The Foundation DR1 includes 225 SNe Ia, 180 of which pass the cuts for inclusion in a cosmological analysis used in Foley et al. (2018) (2 Foundation SNe Ia are at $z > 0.1$ and are therefore excluded here).

2.1. Sample Selection Requirements using SALT2

We infer distances from the SNe Ia in the Pantheon and Foundation samples using the most recent version of the SALT2 light curve fitter (Guy et al. 2007) (SALT2.4; Betoule et al. 2014; Guy et al. 2010) and the Tripp estimator (Tripp 1998):

$$\mu = m_B - \mathcal{M} + \alpha \times x_1 - \beta \times c. \quad (1)$$

m_B is the log of the light curve amplitude, x_1 is the light curve shape parameter, and c is the light curve color parameter. α and β are nuisance parameters along with \mathcal{M} , a parameter encompassing the SN Ia absolute magnitude at peak and the Hubble constant.

The Pantheon and Foundation analyses apply sample selection criteria using these SALT2 light curve parameters to ensure that the SN Ia included can yield accurate distances. These include cuts on the shape and color to ensure that the SNe are within the parameter ranges for which the SALT2 model is valid ($-3 < x_1 < 3$, $-0.3 < c < 0.3$), and cuts to ensure that the shape and time of maximum light are well-measured (x_1 uncertainty < 1 day and time of maximum uncertainty < 2 days). Here, we also require Milky Way reddening of $E(B - V) < 0.15$ mag and $z > 0.01$ to remove SNe with large systematic peculiar velocity uncertainties.

The Foundation data have a few additional selection criteria, all of which were applied in Foley et al. (2018): the first light curve point must have a phase of < 7 days, at least 11 total light curve points are required in $griP_1$, and Chauvenet’s criterion is applied to remove outliers. All samples remove spectroscopically peculiar SNe Ia (apart from 1991T-like SNe, which are included).

Finally, survey selection effects bias the SN distances, the light curve shapes, and the light curve colors. We apply bias corrections to the distances and light curve parameters using the BEAMS with Bias Corrections (BBC) method (Kessler & Scolnic 2016). The BBC method uses simulated SN samples to correct x_1 , c , m_B , α , and β for observational biases and selection effects. Though the BBC method makes no corrections based on host galaxy information directly, the BBC corrections are important for this study because SN Ia light curve demographics depend on host properties (Childress et al. 2013) and SNe Ia

with $c < -0.2$ and $x_1 > 2$ have mean Hubble residuals, before BBC correction, of up to 0.2-0.3 mag (Scolnic & Kessler 2016). These residuals are 3-4 times larger than the host mass step.

We use the simulations from Scolnic et al. (2018) and Foley et al. (2018) with the BBC method to generate these bias corrections (Scolnic et al. 2018, in prep, will contain additional simulation details specific to the Foundation sample). The BBC method removes 6 additional SNe from the sample; 3 from Pantheon and 3 from Foundation. We cannot be certain that the bias corrections are valid for these 6 SNe as they lie in a region of shape, color and redshift space that is not well sampled by the SN simulation. With the BBC method, we find $\alpha = 0.141$ and $\beta = 3.149$ using the $z < 0.1$ SNe in this analysis.

After these additional cosmology cuts, 170 $z < 0.1$ SNeIa are from the CSP or CfA surveys, 43 are from SDSS or PS1, and 170 are from the Foundation DR1 sample for a total of 383 SNeIa. We note that Foley et al. (2018) lists 180 SNe as passing all cosmology cuts. Of these, 3 are at $z < 0.01$, 2 are at $z > 0.1$, 2 do not pass cuts due to small changes in the SALT2 fitting parameters¹³ and the remainder are lost due to BBC cuts. See Foley et al. (2018) and Scolnic et al. (2018) (and references therein) for additional details on the sample selection.

2.2. Sample Selection Requirements using Host Galaxy Properties

We measure host galaxy properties with photometry from the PS1 first data release (Chambers et al. 2016) and the Sloan Digital Sky Survey Data Release 14 (SDSS DR14; Abolfathi et al. 2017). The PS1 DR1 has deep, *grizy* observations over 3π steradians of the sky and has observed at the locations of over 90% of SNe in the current low- z sample. PS1 y band photometry in particular allows for a robust determination of host galaxy masses. SDSS has imaged $\sim 14,000$ square degrees in the *ugriz* filters, including the locations of $\sim 65\%$ of the SNe in the Pantheon+Foundation low- z sample. We measure SDSS u and PS1 *grizy* photometry within apertures of 3 kpc diameter at the location of each SN in this sample.

To observe only the regions within ~ 3 kpc of the SN, we require the typical seeing of PS1 and SDSS to correspond to 3 kpc in physical size or less. PS1 images have a typical seeing of $\sim 1''$, while SDSS images have a median seeing of approximately $1.38''$ in u . Blending of local and global effects may occur at higher redshifts. If we therefore restrict our sample to $z < 0.1$, where 3 kpc corresponds to an angle of $\sim 1.6''$, we can be assured that we are indeed probing local regions.

We also remove 29 SNe in galaxies with inclination angles $> 70^\circ$ based on the Tully & Fisher (1977) axial ratio method, leaving 354. This cut increases the likelihood that local regions are truly local, as highly inclined galaxies could have non-local regions contained in the 3 kpc aperture due to projection effects. However, we note that projection effects will always be a concern in this type of study, particularly in early-type galaxies. Finally, we remove SNe for which the identifi-

cation of the host galaxy is uncertain. SNe for which the host cannot be reliably identified should not be used in a sample that compares local to global measurements. We match SNeIa to candidate host galaxies using the galaxy size- and orientation-weighted SN separation parameter, R (Sullivan et al. 2006):

$$\begin{aligned} R^2 &= C_{xx}x_r^2 + C_{yy}y_r^2 + C_{xy}x_r y_r \\ C_{xx} &= \cos^2(\theta)/r_A^2 + \sin^2(\theta)/r_B^2 \\ C_{xy} &= 2 \cos(\theta) \sin(\theta)(1/r_A^2 + 1/r_B^2) \\ C_{yy} &= \sin^2(\theta)/r_A^2 + \cos^2(\theta)/r_B^2, \end{aligned} \quad (2)$$

where $x_r = x_{SN} - x_{gal}$ and $y_r = y_{SN} - y_{gal}$. r_A , r_B , and θ are galaxy ellipse parameters measured by SExtractor (Bertin & Arnouts 1996). Each R parameter corresponds to an elliptical radius about the host center. We consider the host ambiguous if the minimum R is greater than 5. This cut removes an additional 83 SNe, leaving a final sample of 273 SNe.

After all cuts, *grizy* images for measuring the local mass step are available for 273 SNeIa. 195 of these SNe lie in the SDSS footprint and therefore have u measurements for measuring the rest-frame $u - g$ color. We do not attempt to infer rest-frame u colors for host galaxies without u observations.

3. MEASURING HOST GALAXY PROPERTIES AND THE HUBBLE RESIDUAL STEPS

The local photometry was measured within a circular aperture of radius 1.5 kpc, while the global host galaxy photometry was measured using elliptical aperture photometry. The size of the global host ellipse was set to be equal to the $R = 4$ ellipse measured by SExtractor on each PS1 r -band image. A uniform ellipse radius that extends just beyond the estimated isophotal radius of the galaxy ensures that all flux is captured and that a uniform aperture size is used for all photometric bands. An $R = 4$ ellipse is still small enough for contamination from neighboring stars or galaxies to be negligible. In addition, the difference between the PS1 and SDSS seeing is just 1.7% of the median $R = 4$ semimajor axis of the galaxies in this sample and therefore should not significantly bias the photometry, especially given that the elliptical aperture extends beyond each galaxy's isophotal radius.

We then fit the local and global *ugrizy* photometry to template SEDs following the method of Pan et al. (2014). We estimate galaxy masses and un-reddened, rest-frame u and g colors using the Z-PEG SED-fitting code (Le Borgne & Rocca-Volmerange 2002), which is based on spectral synthesis from PEGASE.2 (Fioc & Rocca-Volmerange 1997). Galaxy SED templates correspond to spectral types SB, Im, Sd, Sc, Sbc, Sa, S0 and E. We marginalize over E(B-V), which is allowed to vary from 0 to 0.2 mag, and the star formation rate. In addition to varying E(B-V), Z-PEG uses 15 star formation histories, 200 stellar age bins, and 6 metallicity bins to fit the observed photometry and densely sample the parameter space.

Uncertainties are estimated by generating Monte Carlo realizations of our photometric measurements. For each filter, we generate mock photometric points from a normal distribution with standard deviation equal to the

¹³ In order to match the Pantheon analysis, we reduce the wavelength range over which the SALT2 model is fit to the photometric data to a maximum of 7000 Å.

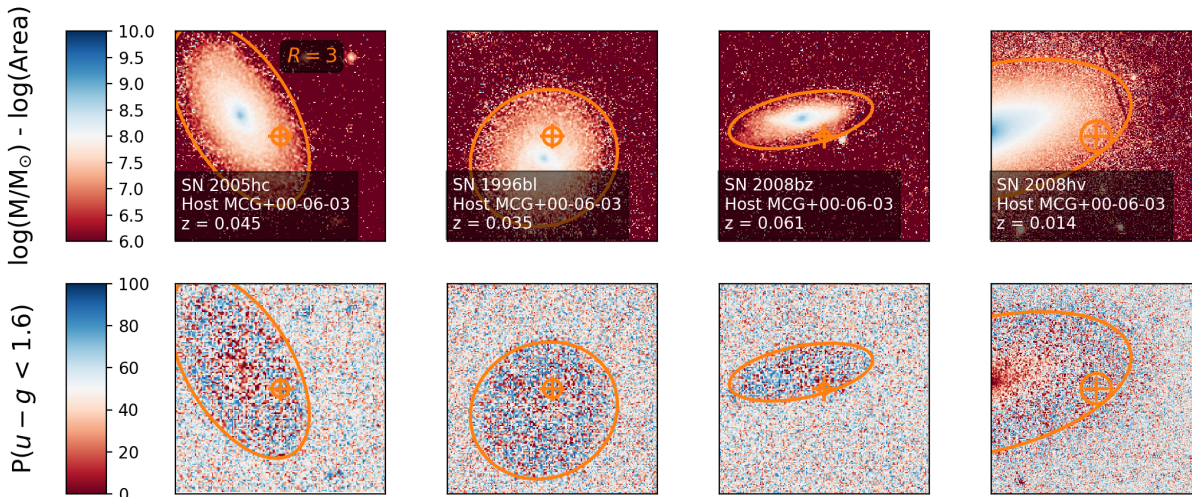


FIG. 1.— Local mass density and $u-g$ maps from four representative galaxies in our sample. The local mass and colors used in this work are measured from the 3 kpc diameter regions indicated by the small circles. For illustration, the local mass density is computed per pixel and has a median value of $\log(M_*/M_\odot) - \log(\text{Area}) \sim 8 \text{ kpc}^{-2}$. To include regions of negative flux in the map, which have an undefined color measurement, the bottom row shows the probability that the true $u-g$ color is < 1.6 mag (the median observed color of this sample). The approximate $R = 3$ isophotal radius of each galaxy is denoted by the ellipses. White colors in the map indicate regions on the border between locally high-mass and low-mass and blue $u-g$ /red $u-g$ (and may also indicate pixels with higher than average noise). For the purposes of this plot, we use observer-frame $u-g$ colors that have not been corrected for host galaxy reddening and Equation 8 from Taylor et al. (2011) to approximate the host galaxy mass using the observed gi photometry.

photometric uncertainties, and use Z-PEG to fit SEDs to each realization of the photometric data. We then estimate the uncertainty in the host mass and rest-frame photometry from the spread in output values. The photometric uncertainties from this approach can occasionally be unrealistically small; for this reason we add 0.05 mag uncertainty in quadrature to the $u-g$ rest-frame colors, approximately equal to the photometric errors for a 3 kpc region in a bright host galaxy, to account for systematic uncertainties in the SED fitting.

Several studies have discussed whether local and global SED-fitting measurements are self-consistent. Sorba & Sawicki (2015) found a 0.1 dex bias in global host galaxy mass measurements of star-forming galaxies when fitting mass to the photometry of the entire galaxy instead of performing a pixel-by-pixel fit and summing the individual measurements. This level of bias will not affect our results, as we look at global and local mass independently (defining the step location separately for global and local measurements). The location of the step is also not known to within 0.1 dex (Scolnic et al. 2018). Other studies have found that summing the results of pixel-by-pixel SED fitting give the same parameters as a SED fit to the photometry of the whole galaxy (Salim et al. 2016; San Roman et al. 2018).

3.1. Measuring the Mass and Color Steps

We treat the dependence of SNIa shape- and color-corrected magnitude on host mass and $u-g$ as a step function, as previous studies have found this to be well-motivated by the data (Betoule et al. 2014; Roman et al. 2018). There may be theoretical reasons to favor a step function as well; Childress et al. (2014) predict that the mean ages of SNIa progenitors undergo a sharp transition between low-mass and high-mass galaxies. If Hubble

residuals depend on physics related to progenitor age, a step would naturally be produced in this model. The dust extinction law in passive versus star-forming galaxies could also change in a way that would produce a step.

To estimate the size of the mass and $u-g$ color steps, we use the maximum likelihood approach from Jones, Riess, & Scolnic (2015). Our likelihood model treats SNe in low-mass and high-mass regions (or in regions with blue/red $u-g$ colors) as belonging to two separate Gaussian distributions and simultaneously determines the maximum likelihood means and standard deviations of those two distributions. The four parameters of this model can be easily constrained with a standard minimization algorithm. The baseline approach considered here does not re-fit α and β on each side of the color or mass split, but we explore this approach in §4.2.

The step between low-mass/high-mass and bluer/redder $u-g$ may correspond roughly to the boundary between passive and star-forming galaxies. The median rest-frame, host galaxy dust-corrected $u-g$ color of this sample is 1.27, and we adopt this value as an agnostic choice for the location of the step following Roman et al. (2018). For the local mass step, we again choose the divide between the locally “low” and “high” mass galaxies to be the median local mass of our sample, $\log(M_*/M_\odot) = 8.83$. The local mass, as defined here, is the stellar mass in the cylinder within a circular aperture of diameter 3 kpc. Unlike the local mass or color steps, the location of the global host mass step has been well-measured by multiple independent datasets and analyses. For this reason, we adopt the standard global host mass step location of $\log(M_*/M_\odot) = 10$ (Sullivan et al. 2010; Betoule et al. 2014; Scolnic et al. 2018). Figure 1 shows local mass per pixel and $u-g$ maps for four representative galaxies in our sample.

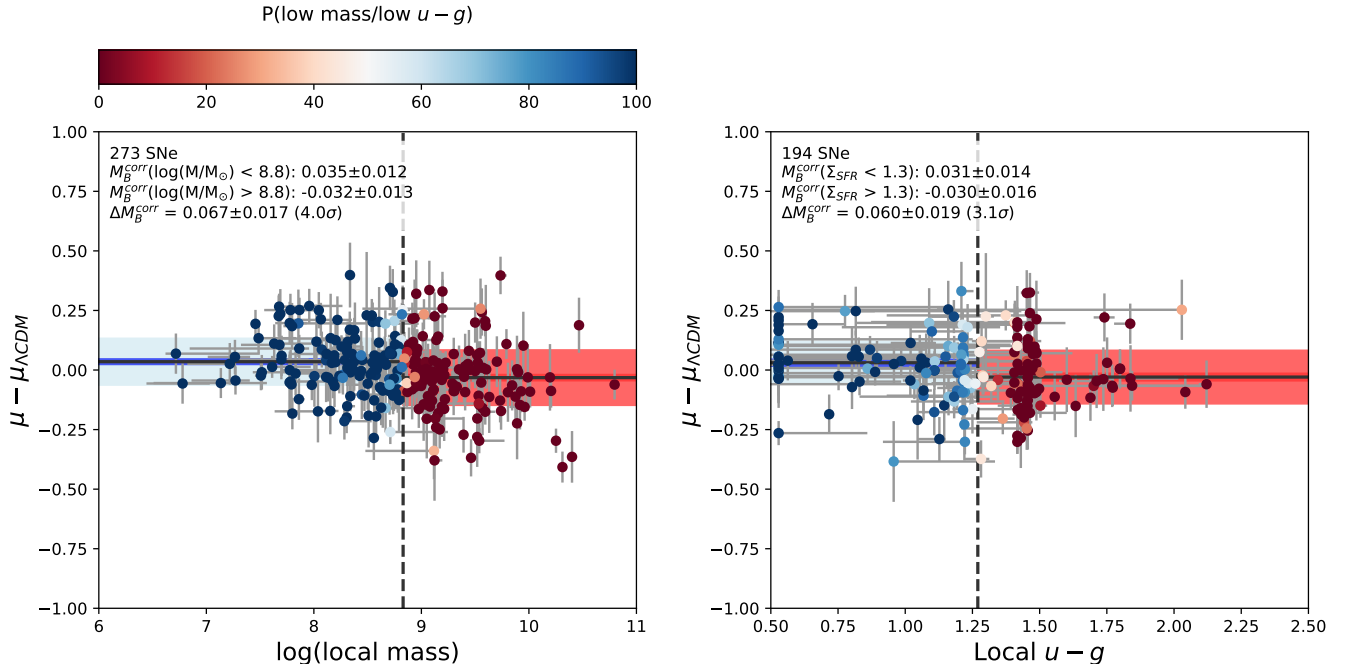


FIG. 2.— The dependence of SN luminosities on the mass and $u-g$ color within 1.5 kpc of the SN location. Colors indicate the probability that a SN is in a low-mass host galaxy (left) or a galaxy with blue rest-frame color (right). We see $\geq 2\sigma$ correlations with both quantities. The gap in rest-frame $u-g$ colors at ~ 1.3 mag is likely due to a gap in the colors of the PEGASE.2 SED templates, the green valley between star-forming and passive host galaxies.

3.2. Measuring the Mass and Color in Random Apertures

We also consider whether the global step is driven by the local step and if so, how “local” the local measurement needs to be (Rigault et al. 2015; Roman et al. 2018). To address this question, we place 150 random apertures of diameter 3 kpc in each galaxy and measure the local mass and $u-g$ color within those apertures. We use the SED template-fitting approach discussed above to fit the photometry in each aperture individually. We use these random measurements to ask whether the region near the SN is better correlated with SN luminosity than the regions far from the SN.

We again use the galaxy size- and orientation-weighted SN separation parameter R to choose where to place the apertures. We first use SExtractor to measure the ellipse that best approximates the shape of a given host galaxy. Each region with a given R parameter lies at the same elliptical radius about the host center. Regions with $R = 0$ are at the host center, while regions with $R = 3$ are approximately at the isophotal limit of the galaxy (shown in Figure 1). Regions with $R = 5$ are outside the isophotal limit of the galaxy and lie far enough away from the host center that identifying the true host galaxy begins to become ambiguous. To include as many apertures near the galaxy center as far from it, we place random apertures so that 25 have $0 < R < 1$, 25 have $1 < R < 2$, and so on out to $R = 5$, which is the Sullivan et al. (2006) criteria for matching a SN to its likely host galaxy.

We use these random measurements to explore how the local mass and color steps change if host properties are inferred from regions far from the SN location. For random apertures with a given distance from the SN location or a given R , we measure the physical properties associ-

ated with each SN from the random location instead of the SN location. We use these random measurements to find the maximum likelihood mass and color steps, and compare to the mass and $u-g$ steps using the properties of the host galaxy at the SN location. For each set of random measurements, we choose the median of those measurements for the step location. This prevents a situation where the vast majority of the sample is on one side of the step location, which can occur as apertures move preferentially towards or away from the host galaxy center.

The spacing of these random apertures will be less than the seeing of the images in most cases, meaning that many random measurements will be partially correlated. However, we can avoid statistical complications by using just one random measurement per SN at a given time and avoiding regions within 3 kpc of the true SN location.

4. RESULTS

Using the methods described above, we measure a local mass step of 0.067 ± 0.017 mag (3.9σ significance) and a local color step of 0.060 ± 0.019 mag (3.0σ). These steps are shown in Figure 2. If we use global properties instead of local to measure the size of the step, we find the global mass step to be 0.058 ± 0.018 mag and the global color step to be 0.061 ± 0.020 mag. The local mass step is slightly larger than the global mass step, while the local $u-g$ step is approximately equal to the corresponding global step.

Table 1 summarizes each global and local step measured from these data, both before and after correcting for the maximum likelihood global mass step of 0.058 ± 0.018 mag. Most significantly, we find a local mass step of 0.056 ± 0.017 mag *after* correcting for the global mass (3.3σ). If we instead correct for the local mass step before measuring the global step, we find a

TABLE 1
MASS AND COLOR STEP MEASUREMENTS FOR TARGETED AND NON-TARGETED SURVEYS

	Δ_M		Δ_{u-g}	
	No Global Mass Corr.	Global Mass Corr. ^a	No Global Mass Corr.	Global Mass Corr. ^a
Local Step	0.067 ± 0.017	0.056 ± 0.017	0.060 ± 0.019	0.034 ± 0.020
– Targeted SNe	0.026 ± 0.027	0.012 ± 0.027	-0.001 ± 0.030	-0.018 ± 0.030
– No Targeted SNe	0.091 ± 0.024	0.083 ± 0.024	0.084 ± 0.028	0.055 ± 0.028
Global Step	0.058 ± 0.018	0.001 ± 0.018	0.061 ± 0.020	0.036 ± 0.020
– Targeted SNe	0.061 ± 0.034	0.003 ± 0.035	-0.019 ± 0.031	-0.032 ± 0.029
– No Targeted SNe	0.049 ± 0.024	-0.009 ± 0.025	0.086 ± 0.028	0.058 ± 0.029

^a The size of each step after applying the maximum likelihood global mass correction of 0.058 ± 0.018 mag.

global mass step of 0.055 ± 0.018 (3.1σ). Table 1 also divides the sample into SNe from surveys that target a pre-selected set of galaxies and those that do not (§4.1 below).

Estimating the statistical significance of the difference between the global and local steps is complicated by the fact that global and local measurements are partially correlated. 65% of the SNe in this sample are either globally and locally high-mass or globally and locally low-mass (77% for local color). To estimate the 1σ uncertainty on the difference between the global and local step *with correlated measurements*, we simulate 1,000 SN samples using our real local and global measurements but with Hubble residuals drawn from a Gaussian centered on 0 and with dispersion equal to the real dispersion of our sample. We find that 68% of the Monte Carlo samples have a local/global difference < 0.017 mag for the mass measurements, and < 0.032 mag for the color measurements. These correspond to the 1σ uncertainties on the local/global difference, and are slightly smaller than the uncertainties that would be obtained just by adding the local and global mass uncertainties in quadrature. With this approach, we find that sizes of the global and local measurements for both mass and color are consistent at the 1σ level. Therefore, the data do not indicate that the local steps are intrinsically more significant than the global steps.

Measuring the local mass step from just the 195 SNe Ia with SDSS u data gives a local mass step of 0.054 ± 0.019 , 0.013 mag less than the step measured from the full sample (not statistically significant). The gap in the dust-corrected, rest-frame $u - g$ colors (Figure 2) is likely due to a gap in the colors of the PEGASE.2 SED templates, likely corresponding to the green valley between passive and star-forming galaxies. The local and global measurements used in this work are available online¹⁴.

We note that the results are somewhat affected by our method of correcting the sample for biases in x_1 and c . The BBC method is a relatively new technique that was applied in the Pantheon cosmological analysis (Scolnic et al. 2018). The biases in x_1 and c caused by sample selection are a clear observational bias that can easily be realized in simulated SN Ia samples and found in real data (Scolnic et al. 2014a; Scolnic & Kessler 2016). The BBC method removes these biases and in doing so reduces the local $u-g$ step by 27% due to the strong dependence of SN Ia shape and color on galaxy properties.

We show this dependence for the sample presented here in Figure 3. The apparent size of the local mass step decreases by just 4%.

4.1. Targeted Versus Untargeted Surveys

Roman et al. (2018) measured a step from $z < 0.1$ SNe Ia that was 0.038 ± 0.034 mag smaller than the step they measured from the full sample, though the difference was not statistically significant. If confirmed, this difference could either be due to a redshift evolution of the local step or differences in low- z versus high- z survey methodology. Specifically, much of the low- z data are from surveys that target a pre-selected set of (usually NGC) galaxies. None of the high- z surveys target pre-selected galaxies. Targeted surveys also collect SNe that are more like the sample of SNe Ia within ~ 40 Mpc that are calibrated by Cepheids and used as a rung on the distance ladder for measuring H_0 . On the other hand, all $z > 0.1$ data used for measuring the dark energy equation of state come from surveys that do not target specific galaxies. It may also be relevant that the CfA and CSP low- z SNe were observed on the Johnson filter system, while Foundation and the $z > 0.1$ data were primarily observed on the Sloan filter system. Because SNe observed on the Sloan filter system have g as the bluest band, there could be differences if host galaxy biases affect SN Ia luminosity in a wavelength-dependent manner.

Because because Foundation data come predominantly from untargeted surveys (Gaia, ASAS-SN, PSST), our data can be used to determine whether SNe from targeted surveys have a different local or global step than SNe from untargeted surveys. Foundation includes some data from targeted surveys only because untargeted surveys would likely discover these SNe if the targeted surveys did not exist (Foley et al. 2018). We therefore treat Foundation as an untargeted survey in this analysis.

In Table 1 we compare the local and global steps measured from $z < 0.1$ SNe in targeted surveys (CfA and CSP) and $z < 0.1$ SNe from surveys that are not targeted (Foundation, PS1, and SDSS). After global mass correction, We see a 2.0σ increase in the local mass step, a 1.8σ increase in the local color step, and a 2.1σ increase in the global color step when untargeted surveys are used instead of targeted surveys. Only the difference in the global mass step is statistically insignificant. These differences are not highly significant but could indicate that the correlation of SN distance with host galaxy properties is sensitive to survey selection effects. In the Appendix, we examine the differences in intrinsic dispersion on ei-

¹⁴ <http://pha.jhu.edu/~djones/localcorr.html>

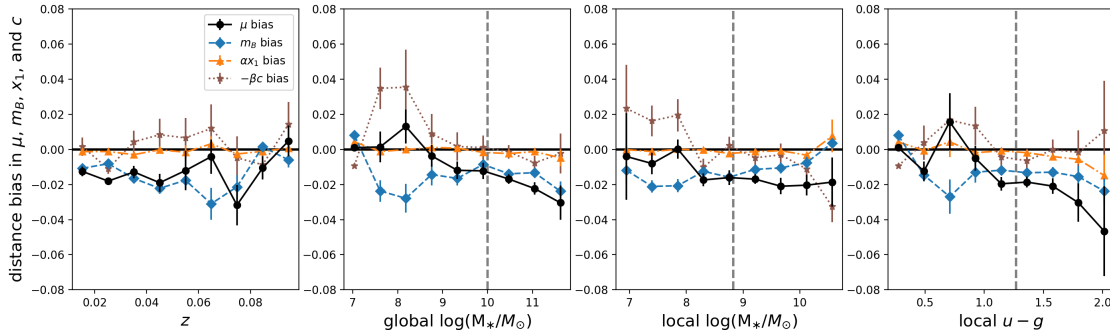


FIG. 3.— The effect of bias corrections on the measured host galaxy steps. In particular, the size of the local color step is 27% larger if the necessary bias corrections are neglected, because SN shape and color are functions of host galaxy $u - g$.

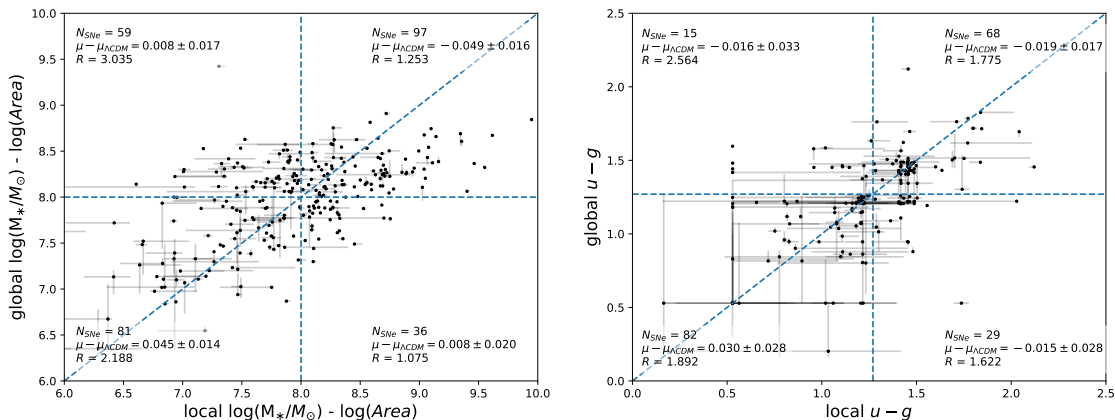


FIG. 4.— Local versus global information for each SN Ia in the sample, where dashed lines indicate the median mass and color along with the points where local measurements equal global measurements. The median Hubble residual for each quadrant is labeled, and shows significant departures from 0 only where local and global agree. Instead of the local and global masses used in this work, we show the mass density, $\log(M_*/M_\odot) - \log(\text{Area})$, where the units of area are kpc and the global mass density is averaged over the total area within the isophotal radius ($R = 3$) of each galaxy.

ther side of the mass and color divide, finding 1-2 σ evidence that SNe in locally low-mass or locally blue regions may have lower dispersions.

One might expect the difference in significance to be affected by the fact that SN Ia in targeted surveys could be biased towards regions with higher stellar mass. Though this is the case for the global mass, it is not the case for the local mass as many SN Ia in the targeted sample are far from the centers of their host galaxies. Of the SN Ia in targeted surveys used in this study, 83% (91 of 110) have global masses > 10 dex, the global mass step divide. However, 51% (56 of 110) occurred in locally massive regions locally massive (local mass > 8.83 dex).

We also check the significance of a local step vs a global step using the Foundation sample alone. Our sample includes 127 Foundation SNe with *grizy* data that can be used to measure the local mass step and 80 Foundation SNe with SDSS *u* observations that can be used to measure the local color step. We find a local mass step of 0.091 ± 0.024 mag (3.8 σ) and a local color step of 0.120 ± 0.030 mag (4.0 σ). We find a global mass step of 0.055 ± 0.027 mag and a global color step of 0.104 ± 0.033 mag, both consistent with the local steps. We find a 2.1 σ difference between the Foundation and non-Foundation local mass step and 2.9 σ difference between the Founda-

tion and non-Foundation local color step.

4.2. Varying Nuisance Parameters

The correlation of SN shape and color may also change as a function of host galaxy properties; β , in particular, could be subject to change due to the change of dust properties as a function of host mass or color. For this reason, we tested the effect of adding separate α and β parameters to the likelihood model for each side of the mass or color step.

The results of α and β variation are shown in Figure 5. We find that α is universally higher in locally red regions and locally massive regions ($\sim 2\sigma$ significance). We find a significant difference in β only for SNe in locally red regions of their host galaxies, which most likely implies that the effect is driven by dust obscuring the SN.

When α and β are allowed to vary, the local mass step increases by 0.005 mag, while the local color step increases by 0.038 mag. Both increases are only marginally significant, but similarly to Rigault et al. (2018), we find that allowing α and β to be fit simultaneously with the local or global step tends to increase the size of the step and reduce the dispersion. We find a dispersion of just 0.047 mag for SNe in locally *red* regions but with a high uncertainty, such that the difference between locally red versus blue regions is not statistically significant. Previ-

TABLE 2
COMBINING LOCAL AND GLOBAL STEPS

	Local Step	Global Step	Combined Step
local mass, global mass	0.059 ± 0.019	0.046 ± 0.021	0.105 ± 0.025
local $u - g$, global $u - g$	0.046 ± 0.028	0.025 ± 0.025	0.070 ± 0.030
local mass, global $u - g$	0.046 ± 0.025	0.046 ± 0.023	0.092 ± 0.031
local $u - g$, global mass	0.030 ± 0.033	0.039 ± 0.032	0.069 ± 0.028

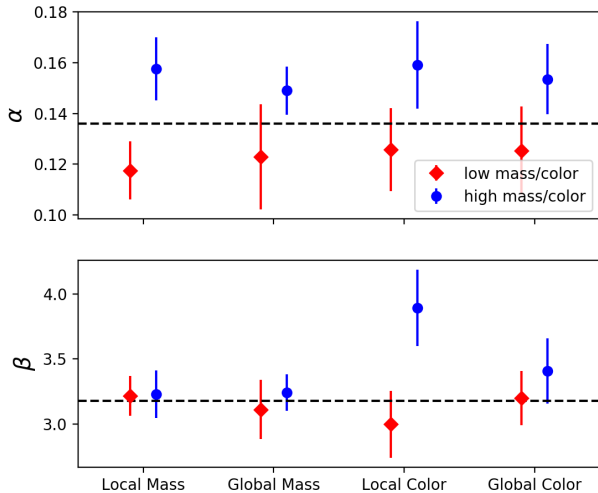


FIG. 5.— The dependence of nuisance parameters α and β on host mass and color. Interestingly, α is measured to be higher in locally/globally red or high-mass hosts. β is higher (nearer to the Milky Way value) for SNe that occurred in redder regions of their host galaxies, likely due to dust effects.

ous results, e.g. Rigault et al. (2015); Kelly et al. (2015) have found lower dispersion in locally *blue* regions, but did not allow α and β to vary (our sample also gives this result at 1σ significance).

4.3. Simultaneously Fitting a Global and Local Step

Table 1 shows that after global mass correction, only the local mass step remains significant at $>3\sigma$ (0.056 ± 0.017 mag). Previous studies (e.g. Roman et al. 2018), have seen a similar effect, which they interpret as evidence that local regions encode information about the SN progenitor that is not captured by a global correction.

In Figure 4 we show the relationship between the local and global measurements in this work to understand which SNe are being corrected by the global versus the local steps. We show the global and local mass densities instead of the global and local mass used elsewhere in this analysis, in order for the local and global units to be the same in this figure. In particular, there are a number of SNe far from the centers of their host galaxies that have high global mass densities but low local mass densities. We label the weighted average of the Hubble residuals in each quadrant. If the local step were driving the global step, we would expect to see a change in Hubble residual only along the x-axis (the local measurement axis). Similarly, if the global measurement were driving the local correction, we would expect the average Hubble residual to change only along the y-axis. Instead, we

see $\sim 4\sigma$ evidence (mass) and $\sim 2.6\sigma$ evidence (color) for a step when considering *only* the two quadrants where local and global agree.

In the previous sections, we have measured only a single step at a time. Beginning with the standard likelihood approach presented in §3, we now expand the method to simultaneously measure a combined local and global step for mass and color. The results are summarized in Table 2. By measuring global and local mass steps together, we find a 3.1σ local mass step and a 2.2σ global mass step. The intrinsic dispersion about the Hubble diagram (the dispersion after photometric uncertainties are taken into account) is 3-5% lower than the dispersion after correcting for a single step. The combined local and global $u - g$ step is less significant than the mass step.

The evidence for a combined local/global mass step is marginally significant, with a Bayesian Information Criterion that is slightly lower ($\Delta\text{BIC} = 3.4$) when an extra step is included in the likelihood model. Making either a global step or local step alone leaves an additional step with $\gtrsim 3\sigma$ significance. Therefore, the possibility that local and global may reinforce each other is intriguing.

4.4. Random Apertures

Having seen evidence for a local mass step after global mass correction, the question remains how “local” the local measurement would need to be to correct SN distances. To answer this question, we use the measurements of mass and color within random apertures discussed in §3.2. We summarize the results of these random tests in Table 3. By inferring local properties from random regions >5 kpc from the SN location after first correcting for the global mass step, we measure a “false local” mass step of 0.029 ± 0.017 mag. This step is smaller than the true local step by 0.027 ± 0.017 mag, a difference with 1.6σ significance. As discussed at the beginning of §4, these uncertainties incorporate the correlation between the local and random measurements. We measure a $u - g$ step of 0.027 ± 0.015 mag, 0.011 ± 0.027 mag smaller than the local step. We therefore see only marginal evidence that measurements of host galaxy properties within 5 kpc of the SN location are important for SN distance corrections. In the Appendix, we examine the differences in intrinsic dispersion between local and random regions, finding no significant difference in dispersion when local mass and color are inferred from random locations instead of locations near the SN.

The last five rows of Table 3 show false local steps using a set of representative R parameters and distances from the SN. *All* of these measurements yield steps smaller than the local step, typically by $\sim 2\sigma$ significance for mass and $\sim 1\sigma$ for color. The R measurements in Table 3 do not include regions within 3 kpc of the SN, so that

TABLE 3
COMPARING LOCAL TO RANDOM MEASUREMENTS

	Δ_M		Δ_{u-g}	
	No Global Mass Corr.	Global Mass Corr. ^a	No Global Mass Corr.	Global Mass Corr. ^a
Local Step	0.067 ± 0.017	0.056 ± 0.017	0.060 ± 0.019	0.038 ± 0.019
Random Step	0.047 ± 0.018	0.029 ± 0.017	0.040 ± 0.020	0.027 ± 0.020
5 kpc from SNe	0.025 ± 0.019	0.000 ± 0.018	0.031 ± 0.021	0.012 ± 0.021
10 kpc from SNe	0.032 ± 0.021	0.015 ± 0.020	0.051 ± 0.021	0.036 ± 0.021
$R < 1$	0.021 ± 0.019	0.002 ± 0.019	0.039 ± 0.023	0.011 ± 0.023
$1 < R < 2$	0.041 ± 0.019	0.018 ± 0.019	0.046 ± 0.021	0.031 ± 0.021
$2 < R < 3$	0.044 ± 0.018	0.021 ± 0.019	0.053 ± 0.020	0.037 ± 0.020

NOTE. — R is the distance from the center of the galaxy in units of the normalized elliptical radius of the galaxy (Sullivan et al. 2006). The last 5 rows exclude regions within 3 kpc of the SN location. Also in the last 5 rows, the step location is taken to be the median of every sample to avoid a situation in which 90% or more of the sample is considered “high-mass” or “low-mass”.

^a The size of each step after applying the maximum likelihood global mass correction of 0.058 ± 0.018 mag.

^b Regions > 5 kpc from SN are randomly sampled. One random region is chosen per SN, the step is measured, and this process is repeated 100 times. The steps listed here are the mean of 100 samples.

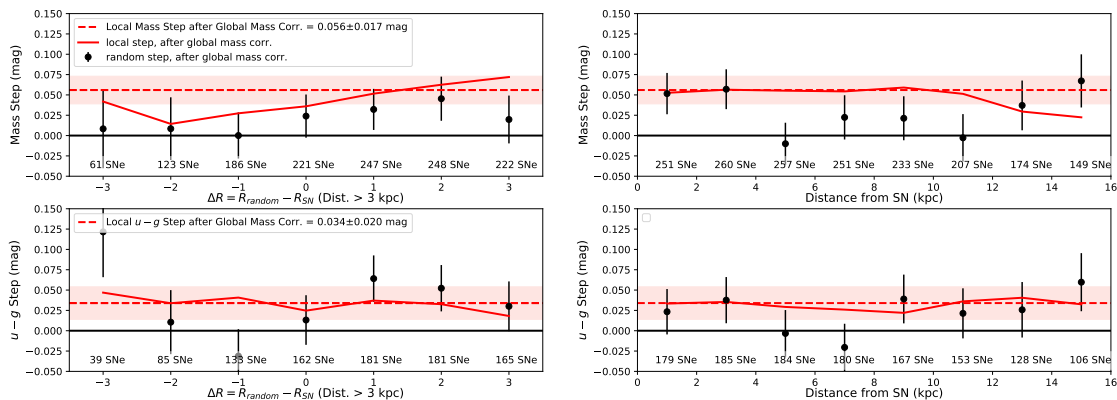


FIG. 6.— After global mass correction, the “false local step” (black): the correlation of SN distance measurements with the masses and $u - g$ colors of different regions in the host galaxy. ΔR is the difference in R between the SN location and the random location after excluding all regions within 3 kpc of the true SN location. The local step after global mass correction and its uncertainty are indicated by the shaded region. For each false local step, the true local step at the SN location (red line) is plotted using the *same set of SNe used to measure the random step*.

no measurements include the true local fluxes at the SN location. We also restrict distance measurements to $R < 5$.

Figure 6 expands the results in Table 3 to show change in the local mass and color steps as a function of both ΔR , the difference in R between the SN and the aperture (left), and of the aperture’s physical distance from the SN (right). Negative ΔR indicates that physical properties are inferred from regions closer to the galactic center than the SN location, while positive ΔR means that the physical properties are inferred from regions farther from the galactic center than the SN location.

As distances from the SNe increase, the sampling of random apertures becomes slightly more sparse and therefore the mass and color steps are not always computed using the full SN sample. There is a similar effect in play for different values of ΔR ; for a SN at the center of its host galaxy, having a random aperture with $\Delta R < 0$ is impossible. Similarly, a SN near the edge of its host could not have a large ΔR . Small hosts in particular will have a restricted range of ΔR and physical distances > 10 kpc from the SN location may be outside

the $R = 5$ ellipse. Therefore, there are significant biases in the global host demographics for different ΔR parameters and distances. For this reason, in Figure 6 we always compare the false local steps to the true local steps measured using the exact same set of SNe.

There are hints that the SN distance measurement becomes less correlated with the localized host galaxy mass at $\gtrsim 5$ kpc from the SN. We also find that a number of mass step measurements are smaller than the local step by $\gtrsim 0.03$ mag ($\sim 2\sigma$). The statistical significance of these differences is limited and different ΔR steps are not completely statistically independent. However, the observed differences between random and local are consistent with the observed 0.056 ± 0.017 mag local mass step after global mass correction. However, we see no statistically significant difference between the local and random color step.

We find a 0.011 mag decrease in the random color step compared to the local color step, which is consistent with Roman et al. (2018). Roman et al. (2018) find a decrease in the size of a local color step of 0.022 mag when changing from their nominal local radius of 3 kpc to a radius of

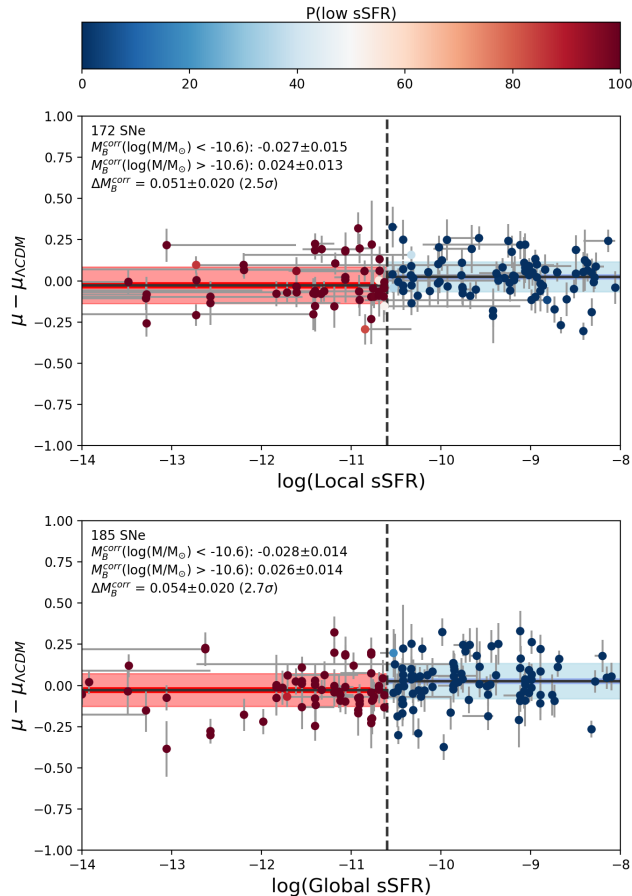


FIG. 7.— Correlation of Hubble residuals with local and global sSFR. We observe steps at $2.5 - 2.7\sigma$ significance, with no significant difference between the local and global steps. After global mass correction, we find a local step of 0.035 ± 0.021 and a global step of 0.029 ± 0.020 .

16 kpc, approximately the maximum distance from the SN location considered here. Because we use only a low- z sample to examine local regions, our uncertainties are larger than those of Roman et al. (2018), and a difference of 0.022 is comparable to the 1σ local color uncertainties. However, the 1σ uncertainties on this test constrain the effect of a non-local measurement to $\lesssim 0.04$ mag.

4.5. Local Specific Star Formation Rate

Recent work from Rigault et al. (2018) has suggested that the local specific star formation rate (LsSFR) has a strong correlation with SNIa residuals in SNFactory data. Though we lack the local $H\alpha$ measurements used by Rigault et al. (2018), $ugriz$ photometry should enable us to investigate whether such a correlation is present in our data, though we caution that $H\alpha$ may be a more robust diagnostic of sSFR.

As Z-PEG has difficulty measuring sSFR in passive galaxies, we use LePHARE (Arnouts & Ilbert 2011) with Bruzual & Charlot (2003) spectral templates as an alternative SED-fitting method to infer LsSFR from our sample. We also use LePHARE for consistency checks on our data in §4.6 below. The SED-fitting parameters from LePHARE are broadly consistent with those from Z-PEG; the median $u - g$ color from LePHARE is within

0.04 mag of the Z-PEG color and the median host galaxy mass is just 0.09 dex lower.

Using the median LsSFR of our sample, -10.6 dex, as the divide between SNIa in low- and high-sSFR regions, we measure a step size of 0.051 ± 0.020 mag (2.5σ). The global sSFR step size is nearly identical, 0.054 ± 0.020 mag (2.7σ). The significance of both steps becomes $< 2\sigma$ after global mass step correction (the local step becomes 0.035 ± 0.021 mag and the global step becomes 0.029 ± 0.020 mag). Rigault et al. (2018) find a step of 0.125 ± 0.023 mag (0.163 ± 0.029 mag after allowing α and β to be fit simultaneously with the step). Their result is statistically inconsistent with ours at the 2.4σ level, though removing the BBC corrections would reduce that discrepancy to 2.1σ . If this discrepancy is not due to statistical fluctuation or unforeseen systematic effects due to differences in sample selection, calibration, or sSFR measurement methods, it may be additional evidence that targeted versus untargeted surveys affect the measured step sizes. Interestingly, the sSFR step sizes we measure do not significantly change if we use only SNe from targeted or untargeted samples.

We show the local and global LsSFR steps in Figure 7 and include the LsSFR measurements from LePHARE in our online data.

4.6. Consistency Checks

In this section we present several consistency checks to validate the SED fitting procedures in this work. The Z-PEG SED fitting method is significantly different than that of Roman et al. (2018), for example, who also base their results on the PEGASE.2 templates but warp those templates to match the observed photometry of galaxies in the SuperNova Legacy Survey fields.

However, 54 SNIa in this sample are also included in Roman et al. (2018). We compare our rest-frame $U - V$ colors and observed $u - g$ colors to those measured by Roman et al. (2018) using their online data. Though we measure $u - g$ colors within a 1.5 kpc radius while Roman et al. (2018) use a 3 kpc radius, we observe a median color of 1.52 mag, just 0.06 mag bluer than that of Roman et al. (2018). Though we use rest-frame $u - g$ colors in this work, after fitting with Z-PEG, we verified that the rest-frame $U - V$ colors were consistent with Roman et al. (2018): we find a median rest-frame $U - V$ color of 0.83 mag compared to 0.77 mag for Roman et al. (2018). If we measure a $U - V$ step instead of a $u - g$ step, we find that the step size increases by just 5 mmag.

Z-PEG returns a set of “pseudo-observed” model magnitudes, which have been reddened and redshifted to match the observed data. These model magnitudes should be close to the observed data if our SED fitting procedure is reliable. For 141 of the 194 SNIa with u observations, the pseudo-observed magnitudes are within the 2σ uncertainties on the local $u - g$ color observations. In reality, there is some additional uncertainty on the model which would increase the statistical agreement between model and data. If we restrict our sample to just these 141 SNIa, we measure a local color step of 0.044 ± 0.022 mag, but consistent with the 0.060 ± 0.019 mag step measured from the full sample.

For the local mass step, a simple consistency check may be performed using the relationship between gi photometry and host galaxy stellar mass given by Taylor et al.

(2011):

$$\log(M_*/M_\odot) = 1.15 + 0.70(g - i) - 0.4M_i, \quad (3)$$

where the absolute i magnitude M_i is estimated using $\Omega_M = 0.3$, $\Omega_\Lambda = 0.7$ and $H_0 = 70 \text{ km s}^{-1} \text{ Mpc}^{-1}$. The uncertainty of the relation is 0.1 dex, which we add in quadrature to the propagated photometric uncertainty.

Although this equation does not k -correct the photometry, it is still a reasonable approximation for these low-redshift data. Using this approximation instead of Z-PEG, we measure a local mass step of 0.077 ± 0.017 mag, consistent with the measurement of 0.067 ± 0.017 mag measured from the full sample.

Lastly, we use the LePHARE SED-fitting software (Arnouts & Ilbert 2011) with Bruzual & Charlot (2003) templates (the version used for the COSMOS mass function; Ilbert et al. 2009) to independently check the mass and color measurements from Z-PEG. We find a median color just 0.04 mag redder than the Z-PEG measurements and a median host mass 0.09 dex smaller than the Z-PEG measurements. LePHARE yields less model-dependent colors than Z-PEG, as it uses the SED templates for k -corrections but interpolates using those k -corrections from the observed magnitudes themselves. We measure local mass and color steps that are consistent with, though slightly smaller than, the Z-PEG measurements: with LePHARE, we measure a nearly identical local mass step of 0.066 ± 0.017 mag and a local color step of 0.047 ± 0.019 mag.

5. IMPACT ON THE HUBBLE CONSTANT

A leading approach for measuring the Hubble Constant, H_0 , calibrates the luminosity of SNe Ia in nearby galaxies using Cepheid variables and compares them to SNe Ia in the Hubble flow (typically $z \gtrsim 0.01 - 0.02$). A potential bias may enter if there are differences in the mean host properties of the two SN samples for some of the host properties considered here.

The determination of H_0 in Riess et al. (2016) corrects the two SN samples for the global mass step using a value of 0.06 mag (Betoule et al. 2014), consistent with the 0.058 ± 0.017 mag global step we measure in this work. After the 0.06 mag global mass step is applied to our sample, instead of the 0.058 mag global mass step determined in §4, we measure residual, local step sizes of 0.055 ± 0.017 mag (mass) and 0.033 ± 0.020 mag (color). Of these, only the local mass step may be considered significant and may indicate a bias. Here we calculate the size of a possible bias in H_0 . We also note that for a local step to resolve the discrepancy between the local measurement and the CMB-inferred value (Planck Collaboration et al. 2015), the effect would also have to be present in SN Ia J-band luminosity (Dhawan et al. 2018).

We use the method developed by Rigault et al. (2015) (and also used in Jones et al. 2015) to calculate the potential bias to H_0 due to a local step. The bias to the Hubble constant due to a local mass step is given by:

$$\log(H_0^{\text{corr}}) = \log(H_0) - \underbrace{\frac{1}{5}(\psi^{HF} - \psi^C)}_{\text{local bias correction}} \times \delta\langle M_B^{\text{corr}} \rangle_{\text{local}}, \quad (4)$$

where $\delta\langle M_B^{\text{corr}} \rangle_{\text{local}}$ is the size of the local step after removing the global step. ψ^{HF} and ψ^C are the fractions of SNe Ia in the Hubble flow and in galaxies with Cepheid observations, respectively, that occurred in locally massive regions of their hosts. We use the recent measurement of $H_0 = 73.48 \pm 1.66$ from Riess et al. (2018) as our baseline. ψ^{HF} is computed using only the SNe in this analysis that are also included in Riess et al. (2016). 16 of 19 total Cepheid calibrators have PS1 imaging, as 3 (SN 2001el, SN 2012fr, and SN 2015F) are too far south for PS1. An additional 2 SNe lack SDSS u imaging (SN 2005cf and SN 2007sr). For these 5 SNe, we use SkyMapper photometry (Wolf et al. 2018) instead of PS1 and SDSS photometry to determine the local masses, global colors, and local colors.

Because the fraction of SNe Ia with local masses above or below the step is fairly well balanced across the Cepheid calibrator and Hubble flow samples, with a fractional sample difference of ~ 0.15 , the effect on H_0 is a small fraction of the step, reducing it by $0.28 \text{ km s}^{-1} \text{ Mpc}^{-1}$. This shift is 17% of the present uncertainty in H_0 . A slightly larger sample difference is seen for local $u - g$ colors. We find that 89.5% of Cepheid calibrators are in $u - g < 1.6$ galaxies. In contrast, $\sim 50.0\%$ of the Hubble flow sample are in $u - g < 1.6$ galaxies. However, because the significance of the local color step (after global mass correction) is just 1.7σ , no correction is warranted.

For the local mass, global mass, local $u - g$ and global $u - g$ steps, Table 4 gives the estimated bias to H_0 using the measurements in this work after a global mass correction. These range from 0.02 to $-0.44 \text{ km s}^{-1} \text{ Mpc}^{-1}$. However, only the local mass step is significant and thus could be considered meaningful.

A caveat to applying even the local mass step correction may be drawn from the differences in steps suggested in the previous section for targeted and non-targeted surveys. Both the Cepheid calibrated and Hubble flow samples used in Riess et al. (2016) came exclusively from targeted surveys in which all local steps with or without the global mass correction applied are smaller and not significant with only $\sim 1\sigma$ confidence. If the present hint of a difference in step sizes between these survey types is established with larger surveys, we would conclude that no additional correction to H_0 would be warranted for these local steps. At present a conservative approach would be to apply half the shift to H_0 and consider half the shift as part of the systematic uncertainty.

An alternative approach to accounting for differences in the host properties of SN samples could be to ensure both samples are homogeneous. For the determination of H_0 using Cepheids to calibrate SNe Ia, it is necessary to select calibrators from late-type galaxies. Placing this same selection criterion on the Hubble flow sample, as done in Riess et al. (2016), has a negligible impact on the uncertainty in H_0 because the number of SNe Ia in late-type hosts in the Hubble flow is much larger than the number of calibrators.

6. CONCLUSIONS

We used up to 273 SNe from the Pantheon and Foundation samples to determine whether the physical properties of the regions near the location of SNe Ia are as correlated with SN light curve parameters and inferred

TABLE 4
PREDICTED CHANGE IN H_0 DUE TO MASS AND COLOR STEPS

	Step Significance ^a	% in Cepheid Calibrators	% in Hubble Flow	ΔH_0 (km s ⁻¹ Mpc ⁻¹)
local mass > 8.83 dex	3.2 σ	36.8	52.1	-0.28
global mass > 10 dex	0.1 σ	47.4	70.0	0.02
local $u - g > 1.27$	1.7 σ	10.5	50.0	-0.44
global $u - g > 1.27$	1.8 σ	26.3	46.5	-0.24
local sSFR < -10.6	1.7 σ	21.1	52.0	-0.37
global sSFR < -10.6	1.4 σ	31.6	52.7	-0.21

NOTE. — We show the effect of applying a local step after correcting for a 0.06 mag mass step following Riess et al. (2016). We note that the H_0 correction appears to be stronger in untargeted surveys of SNe Ia than it does in targeted surveys such as the (Riess et al. 2016) sample. Note that the “global mass” correction increases H_0 , as we measure a slightly smaller mass step of 0.058 mag in this work. However, the steps applied are nearly identical to those listed in the “Global Mass Corr.” columns of Table 1.

^a Significance of the step after 0.06 mag correction based on global mass.

SN distances as global host properties or random regions within those same host galaxies. This sample is $\sim 40\%$ larger than the low- z sample used in recent measurements of cosmological parameters. Our measurements of local masses and local, rest-frame $u - g$ colors for the full sample are available online¹⁵.

We see a significant correlation between local stellar mass and SN distance residuals. The presence of a 0.056 ± 0.017 mag local mass step after global mass correction is compelling evidence that local effects should be explored in future analyses. However, even with the largest sample of $z < 0.1$ SNe Ia to date, were unable to definitively prove that local information is better-correlated with SN Ia distance measurements than global or random information. We found just 1.6 σ evidence that SN Ia Hubble residuals were better correlated with local information than with random information inside the same host galaxy.

We find evidence for a correlation between Hubble residuals of SNe for which local and global measurements agree. The difference between the inferred distances of SNe in both locally high-mass regions and globally high-mass galaxies versus those in locally/globally low-mass regions is 0.105 ± 0.025 mag. The evidence that such an effect exists is not definitive, but is plausible given that correcting for a single local or global mass step leaves an additional step with $\sim 3\sigma$ significance. In a sample of SNe Ia for which global and local indicators disagree, we see *no evidence* for a local or global step as a function of either mass or color. Figure 4 summarized the Hubble residuals in each local versus global quadrant. We find 1.7 σ evidence for a local $u - g$ step after correcting for a global host mass step.

Though the results here do not prove that SNe Ia are more correlated with their local host environments than their global environments, we use these results and their uncertainties to put limits on the estimated bias to cosmological parameters due to local effects. The only step detected at $>2\sigma$ significance, the local mass step, would give an estimated systematic shift in H_0 of -0.14 km s⁻¹ Mpc⁻¹ with an additional uncertainty of 0.14 km s⁻¹ Mpc⁻¹, $\sim 10\%$ of the current uncertainty on H_0 .

Lastly, we find 2.1-2.9 σ evidence for tension between measurements of the local step from surveys that target a pre-selected set of galaxies (the previous low- z sample)

and surveys that do not. Previous work has also shown that different samples may have different step sizes and it is not clear why (e.g. Rest et al. 2014; Scolnic et al. 2014b). Roman et al. (2018) found that the targeted low- z sample has marginal evidence for a local color step of 0.049 ± 0.046 mag (1.1 σ significance), but they found a local step that was nearly twice as large when including data with 87% of SNe from untargeted surveys (7.0 σ significance). The fact that the untargeted surveys here were observed on the Sloan filter system, while the targeted surveys used Johnson filters may also perhaps play a role. Though the samples included in Roman et al. (2018) cannot determine whether this result is due to redshift evolution of the step or survey-specific effects, our data – and future Foundation data releases – can break this degeneracy.

We remain agnostic about the reasons for sample-to-sample differences, but it is clear that pre-selecting galaxies will alter the demographics of the SN sample and therefore may change the measured relationships of SNe Ia with their hosts. As most SNe used in the Riess et al. (2016) H_0 measurement are from targeted searches, it is unclear whether it is appropriate to apply a correction to the current H_0 analysis if that correction is measured from untargeted samples. This question is unlikely to be resolved without a better understanding of the relationships between SNe Ia and their environments.

The existing low- z sample is also subject to significant calibration uncertainties and selection biases. A local mass step in particular could be biased by difference imaging residuals in SN Ia photometry. In Foundation, we have multiple epochs of PS1 3π with no SN light that can be used to test and correct for the possibility of small difference imaging biases in future work. When SNfactory (Aldering et al. 2002) and the Foundation second data release are publicly available, these data may reveal correlations that our data are unable to probe.

As the connection between SN environments and their progenitors remains unclear, the SN-host relation will remain a possible source of systematic uncertainty in cosmological analyses for the foreseeable future. If future studies find evidence for a relationship between SN Ia corrected magnitudes and their local environments, we propose that these studies adopt the methodology presented here to determine the “locality” of the correlation. If global host properties will be sufficient to correct SN Ia magnitudes for host galaxy biases, space-based imaging will not be needed for precision cosmology. If, on the

¹⁵ The data are available at <http://pha.jhu.edu/~djones/localcorr.html>.

TABLE 5
MEASUREMENTS OF THE HUBBLE RESIDUAL DISPERSION FOR TARGETED AND NON-TARGETED SURVEYS

	Δ_M			Δ_{u-g}		
	$\log(M_*/M_\odot < 8.9)$	$\log(M_*/M_\odot > 8.9)$	diff.	$u - g < 1.6$	$u - g > 1.6$	diff.
Local Step	0.093 ± 0.010	0.118 ± 0.011	-0.025 ± 0.015	0.108 ± 0.009	0.048 ± 0.043	0.060 ± 0.044
– Targeted SNe	0.067 ± 0.018	0.102 ± 0.026	-0.035 ± 0.032	0.084 ± 0.016	0.000 ± 0.063	0.084 ± 0.065
– No Targeted SNe	0.101 ± 0.013	0.128 ± 0.015	-0.026 ± 0.020	0.122 ± 0.012	0.072 ± 0.042	0.050 ± 0.044
Global Step	0.106 ± 0.013	0.111 ± 0.009	-0.005 ± 0.015	0.107 ± 0.009	0.078 ± 0.042	0.029 ± 0.043
– Targeted SNe	0.089 ± 0.034	0.081 ± 0.015	0.008 ± 0.037	0.085 ± 0.016	0.000 ± 0.047	0.085 ± 0.050
– No Targeted SNe	0.115 ± 0.016	0.127 ± 0.012	-0.012 ± 0.020	0.119 ± 0.012	0.107 ± 0.044	0.012 ± 0.045

NOTE. — Similar to Table 1, except that after correcting for global host galaxy mass we give the measurements of SNIa intrinsic dispersion for subsamples of SNIa in different local or global environments. We measure dispersion using free parameters in the likelihood model presented in §3.1.

TABLE 6
MEASUREMENTS OF THE HUBBLE RESIDUAL DISPERSION AFTER CORRECTING SNIa FOR THEIR LOCAL OR RANDOM ENVIRONMENTS

	Δ_M			Δ_{u-g}		
	$\log(M_*/M_\odot < 8.9)$	$\log(M_*/M_\odot > 8.9)$	diff.	$u - g < 1.6$	$u - g > 1.6$	diff.
Local Step	0.094 ± 0.016	0.116 ± 0.027	-0.022 ± 0.031	0.089 ± 0.015	0.115 ± 0.014	-0.026 ± 0.020
Random Step ^a	0.084 ± 0.009	0.127 ± 0.012	-0.043 ± 0.015	0.096 ± 0.015	0.112 ± 0.014	-0.016 ± 0.021
5 kpc from SNe	0.101 ± 0.012	0.119 ± 0.016	-0.018 ± 0.020	0.087 ± 0.013	0.127 ± 0.015	-0.040 ± 0.020
10 kpc from SNe	0.110 ± 0.012	0.114 ± 0.012	-0.004 ± 0.017	0.101 ± 0.015	0.109 ± 0.014	-0.009 ± 0.021
$R < 1$	0.094 ± 0.011	0.110 ± 0.012	-0.015 ± 0.016	0.074 ± 0.015	0.128 ± 0.018	-0.055 ± 0.024
$1 < R < 2$	0.101 ± 0.010	0.120 ± 0.012	-0.020 ± 0.016	0.094 ± 0.013	0.118 ± 0.014	-0.024 ± 0.019
$2 < R < 3$	0.087 ± 0.011	0.129 ± 0.012	-0.042 ± 0.016	0.092 ± 0.015	0.118 ± 0.014	-0.026 ± 0.021

NOTE. — Similar to Table 3, except that but we give the measurements of SNIa intrinsic dispersion for subsamples of SNIa using the likelihood model presented in §3.1 (after correcting for host galaxy mass). We explore how the difference in dispersion between samples of SNIa with different host characteristics evolves when SNIa properties are inferred from random regions or regions far from the SN location.

^a Regions >5 kpc from SN are randomly sampled. One random region is chosen per SN, the step is measured, and this process is repeated 100 times. The steps listed here are the mean of 100 samples.

other hand, convincing evidence is shown that regions 5 kpc from the SN location are not as well correlated with the SNIa corrected magnitude as regions 2 kpc from the SN location, this would have enormous consequences for future cosmological analyses and the resources such analyses would require.

We would like to thank the anonymous referee for many helpful suggestions to improve this manuscript. We would also like to thank Marcin Sawicki, Mickael

Rigault, and Ravi Gupta for their assistance in improving the measurements and text. D.O.J. is supported by a Gordon and Betty Moore Foundation postdoctoral fellowship at the University of California, Santa Cruz. The UCSC group is supported in part by NASA grant NNG17PX03C, NSF grant AST-1518052, the Gordon & Betty Moore Foundation, the Heising-Simons Foundation, and by fellowships from the Alfred P. Sloan Foundation and the David and Lucile Packard Foundation to R.J.F.

APPENDIX

INTRINSIC DISPERSION MEASUREMENTS FOR EACH SUBSAMPLE

In this appendix, we reproduce Tables 1 and 3 but list dispersion values instead of mass and color step measurements for each subsample (Tables 5 and 6). We measure these dispersions using the likelihood model presented in §3.1. Occasionally, dispersions are equal to zero, but with high uncertainty meaning that photometric errors alone appear to explain the scatter about the Hubble diagram.

We see $\sim 1 - 2\sigma$ evidence that SNe Ia in locally low-mass or locally blue regions have lower dispersion. However, we do not see a significant difference between the “local” and “random” measurements for the dispersion.

REFERENCES

- Abolfathi, B., Aguado, D. S., Aguilar, G., et al. 2017, ArXiv e-prints
Aldering, G., Adam, G., Antilogus, P., et al. 2002, in Society of Photo-Optical Instrumentation Engineers (SPIE) Conference Series, Vol. 4836, Survey and Other Telescope Technologies and Discoveries, ed. J. A. Tyson & S. Wolff, 61–72
Arnouts, S., & Ilbert, O. 2011, LePHARE: Photometric Analysis for Redshift Estimate, Astrophysics Source Code Library
Bertin, E., & Arnouts, S. 1996, A&AS, 117, 393
Betoule, M., Kessler, R., Guy, J., et al. 2014, A&A, 568, A22
Bruzual, G., & Charlot, S. 2003, MNRAS, 344, 1000
Chambers, K. C., Magnier, E. A., Metcalfe, N., et al. 2016, ArXiv e-prints

- Childress, M., Aldering, G., Antilogus, P., et al. 2013, *ApJ*, 770, 108
- Childress, M. J., Wolf, C., & Zahid, H. J. 2014, *MNRAS*, 445, 1898
- Contreras, C., Hamuy, M., Phillips, M. M., et al. 2010, *AJ*, 139, 519
- Dhawan, S., Jha, S. W., & Leibundgut, B. 2018, *A&A*, 609, A72
- Fioc, M., & Rocca-Volmerange, B. 1997, *A&A*, 326, 950
- Folatelli, G., Phillips, M. M., Burns, C. R., et al. 2010, *AJ*, 139, 120
- Foley, R. J., Scolnic, D., Rest, A., et al. 2018, *MNRAS*, 475, 193
- Gaia Collaboration, Prusti, T., de Bruijne, J. H. J., et al. 2016, *A&A*, 595, A1
- Graur, O., Bianco, F. B., & Modjaz, M. 2015, *MNRAS*, 450, 905
- Guy, J., Astier, P., Baumont, S., et al. 2007, *A&A*, 466, 11
- Guy, J., Sullivan, M., Conley, A., et al. 2010, *A&A*, 523, A7
- Hayden, B. T., Gupta, R. R., Garnavich, P. M., et al. 2013, *ApJ*, 764, 191
- Hicken, M., Wood-Vasey, W. M., Blondin, S., et al. 2009a, *ApJ*, 700, 1097
- Hicken, M., Challis, P., Jha, S., et al. 2009b, *ApJ*, 700, 331
- Hicken, M., Challis, P., Kirshner, R. P., et al. 2012, *ApJS*, 200, 12
- Holoien, T. W.-S., Brown, J. S., Stanek, K. Z., et al. 2017, *MNRAS*, 471, 4966
- Huber, M., Chambers, K. C., Flewelling, H., et al. 2015, *The Astronomer's Telegram*, 7153
- Ilbert, O., Capak, P., Salvato, M., et al. 2009, *ApJ*, 690, 1236
- Jha, S., Kirshner, R. P., Challis, P., et al. 2006, *AJ*, 131, 527
- Jones, D. O., Riess, A. G., & Scolnic, D. M. 2015, *ApJ*, 812, 31
- Jones, D. O., Scolnic, D. M., Riess, A. G., et al. 2018, *ApJ*, 857, 51
- Kelly, P. L., Filippenko, A. V., Burke, D. L., et al. 2015, *Science*, 347, 1459
- Kelly, P. L., Hicken, M., Burke, D. L., Mandel, K. S., & Kirshner, R. P. 2010, *ApJ*, 715, 743
- Kessler, R., & Scolnic, D. 2016, *ArXiv e-prints*
- Kessler, R., Becker, A. C., Cinabro, D., et al. 2009, *ApJS*, 185, 32
- Kim, Y.-L., Smith, M., Sullivan, M., & Lee, Y.-W. 2018, *ArXiv e-prints*
- Lampeitl, H., Smith, M., Nichol, R. C., et al. 2010, *ApJ*, 722, 566
- Le Borgne, D., & Rocca-Volmerange, B. 2002, *A&A*, 386, 446
- Maoz, D., Mannucci, F., & Nelemans, G. 2014, *ARA&A*, 52, 107
- Pan, Y.-C., Sullivan, M., Maguire, K., et al. 2014, *MNRAS*, 438, 1391
- Planck Collaboration, Ade, P. A. R., Aghanim, N., et al. 2015, *ArXiv e-prints*
- Rest, A., Scolnic, D., Foley, R. J., et al. 2014, *ApJ*, 795, 44
- Riess, A. G., Kirshner, R. P., Schmidt, B. P., et al. 1999, *AJ*, 117, 707
- Riess, A. G., Macri, L. M., Hoffmann, S. L., et al. 2016, *ApJ*, 826, 56
- Riess, A. G., Casertano, S., Yuan, W., et al. 2018, *ApJ*, 855, 136
- Rigault, M., Copin, Y., Aldering, G., et al. 2013, *A&A*, 560, A66
- Rigault, M., Aldering, G., Kowalski, M., et al. 2015, *ApJ*, 802, 20
- Rigault, M., Brinnet, V., Aldering, G., et al. 2018, *ArXiv e-prints*
- Rodney, S. A., Riess, A. G., Strolger, L.-G., et al. 2014, *AJ*, 148, 13
- Roman, M., Hardin, D., Betoule, M., et al. 2018, *A&A*, 615, A68
- Salim, S., Lee, J. C., Janowiecki, S., et al. 2016, *ApJS*, 227, 2
- San Roman, I., Sánchez-Blázquez, P., Cenarro, A. J., et al. 2018, *ArXiv e-prints*
- Schlafly, E. F., Finkbeiner, D. P., Jurić, M., et al. 2012, *ApJ*, 756, 158
- Scolnic, D., & Kessler, R. 2016, *ArXiv e-prints*
- Scolnic, D., Rest, A., Riess, A., et al. 2014a, *ApJ*, 795, 45
- Scolnic, D. M., Riess, A. G., Foley, R. J., et al. 2014b, *ApJ*, 780, 37
- Scolnic, D. M., Jones, D. O., Rest, A., et al. 2018, *ApJ*, 859, 101
- Sorba, R., & Sawicki, M. 2015, *MNRAS*, 452, 235
- Stritzinger, M. D., Phillips, M. M., Boldt, L. N., et al. 2011, *AJ*, 142, 156
- Sullivan, M., Le Borgne, D., Pritchett, C. J., et al. 2006, *ApJ*, 648, 868
- Sullivan, M., Conley, A., Howell, D. A., et al. 2010, *MNRAS*, 406, 782
- Sullivan, M., Guy, J., Conley, A., et al. 2011, *ApJ*, 737, 102
- Taylor, E. N., Hopkins, A. M., Baldry, I. K., et al. 2011, *MNRAS*, 418, 1587
- Tonry, J. L., Denneau, L., Heinze, A. N., et al. 2018, *ArXiv e-prints*
- Tripp, R. 1998, *A&A*, 331, 815
- Tully, R. B., & Fisher, J. R. 1977, *A&A*, 54, 661
- Uddin, S. A., Mould, J., Lidman, C., Ruhlmann-Kleider, V., & Zhang, B. R. 2017, *ApJ*, 848, 56
- Wolf, C., Onken, C. A., Luvaul, L. C., et al. 2018, *PASA*, 35, e010